Nat Hazards (2015) 77:693–716
DOI 10.1007/s11069-015-1617-x

ORIGINAL PAPER

Lahar simulation at active volcanoes of the Southern Andes: implications for hazard assessment

Angelo Castruccio · Jorge Clavero

Received: 17 July 2014 / Accepted: 10 January 2015 / Published online: 21 January 2015

Abstract Lahars are catastrophic events that have the potential to cause the loss of life and damage to infrastructure over inhabited areas. Consequently the zoning of associated hazards is a critical task. We evaluated the lahar hazards at two volcanoes of the Southern Volcanic Zone of the Andes of Chile: Villarrica and Calbuco. We applied the LAHARZ and MSF codes using three DEMs: SRTM, ASTER GDEM and a topographic map-derived DEM to evaluate whether low-resolution and widely available DEMs are suitable for modelling lahars. Our results indicate that the original 0.05 calibration constant used in the original global LAHARZ model to calculate the cross-sectional area of inundation is not adequate for lahars from these volcanoes, and our analyses suggest a value of 0.02 as a more appropriate value. One of the most important results obtained is the high relevance that simulating topographic changes for multi-pulses lahar events has. The simulations indicate that dramatic changes in trajectories could occur during such scenarios, and areas not recognized as susceptible of being affected by lahars using the original topography can also be affected. These results have important implications for hazard assessment, as for example, the town of Pucón, located 16 km to the N of the Villarrica volcano was not recognized to be located in inundation areas when using LAHARZ on the original topography represented by unmodified DEMs. However, more than 50 % of the town could be inundated if lahars are modelled as multiple pulses, in agreement with geological and historical observations, as well as results shown on previous hazard maps. The MSF code better simulates the lateral extension of possible lahars, especially over flat areas or

Electronic supplementary material The online version of this article (doi:10.1007/s11069-015-1617-x) contains supplementary material, which is available to authorized users.

A. Castruccio (✉)
Departamento de Geología, Universidad de Chile, Plaza Ercilla 803, Casilla, 13518 Santiago, Chile
e-mail: acastruccio@gmail.com; acastruc@ing.uchile.cl

A. Castruccio
Centro de Excelencia en Geotermia de los Andes (CEGA), FONDAP 15090013, Santiago, Chile

J. Clavero
Escuela de Geología, Universidad Mayor, Santiago, Chile

where topography is complex with many stream trajectories, but lacking a reliable method to determine the run-out distance. Our results indicate that the modifications made to the LAHARZ governing equations give very good results for assessing the hazards associated with lahars in volcanoes of this region of the Andes.

Keywords Lahars · Hazard assessment · Computer modelling · Southern Andes

1 Introduction

Lahars are gravity-driven flows, composed essentially of a mixture of volcanic sediments and water that advance down volcanic slopes. They constitute one of the most hazardous and destructive volcanic processes as a result of their high energy and mobility, costing more than 30,000 lives during the twentieth century (Major and Newhall 1989; Vallance 2000). The Southern Volcanic Zone (SVZ) of the Andes extends from 33°S to 48°S (e.g. Stern et al. 2007) where more than 80 % of Chile's population is concentrated. Because of their latitude positions, related with climate factors and the high heights of most of the volcanic centres of this zone, the main active volcanoes tend to be permanently covered by glacial ice and snow (e.g. Rivera et al. 2008). This potential supply of water makes lahars the most likely and hazardous volcanic phenomena in this region of the Andes. During historical eruptions in the SVZ, lahars have been the most recurrent volcanic hazard, causing most of the twentieth century's eruption-related fatalities and destruction (e.g. Calbuco 1961, Villarrica 1971, Llaima 2008, Chaitén 2008; see González 1995; Naranjo and Moreno 2004; Pierson et al. 2013).

Due to the high frequency and destructiveness of lahars in the SVZ and the increasing population of the surrounding areas (Stern et al. 2007), it is essential to make better maps of the hazard zones associated with lahars for all the volcanoes that can affect populated areas. These studies will certainly help local authorities in order to take proper preventive actions prior to and during an eruptive event. Traditionally, hazard assessment has been based on an empirical method through detailed fieldwork in order to estimate the frequency and extension of different types of past volcanic processes (e.g. Moreno 1999, 2000). However, limiting factors such as changes in topography since last eruptions, the possibility of occurrence of volcanic processes not previously recorded in the history of a particular volcano, the difficulty of access to some areas and the need of a quick response to a volcanic crisis has prompted volcanologists to seek alternative methods for determining and mapping these hazards.

Computer models have been used intensively in the last decades to evaluate and map hazards associated with lava flows, pyroclastic flows, ash fall and lahars (e.g. Felpeto et al. 2007; Macedonio et al. 2008; Vicari et al. 2009). These models use different approaches to simulate the extension and characteristics, and sometimes the dynamics, of the flows associated with each hazard. These approaches vary from statistical–empirical data-based models with correlation parameters that do not take into account the physics of volcanic processes (e.g. LAHARZ; Schilling 1998), to very complex ones that take into account the physical and environmental variables needed to derive and solve governing equations (e.g. TITAN2D; Patra et al. 2006).

Among the existing models to simulate lahars, LAHARZ (Schilling 1998) has been the most widely used (e.g. Muñoz-Salinas et al. 2009; Worni et al. 2012) due to its ease of use

and widely availability and the minimal input data required. Recently, a revised version of LAHARZ has been published (Schilling 2014), which includes an updated ARCGIS menu-driven interface and options to merge resulting inundation zones, vectorizing inundation

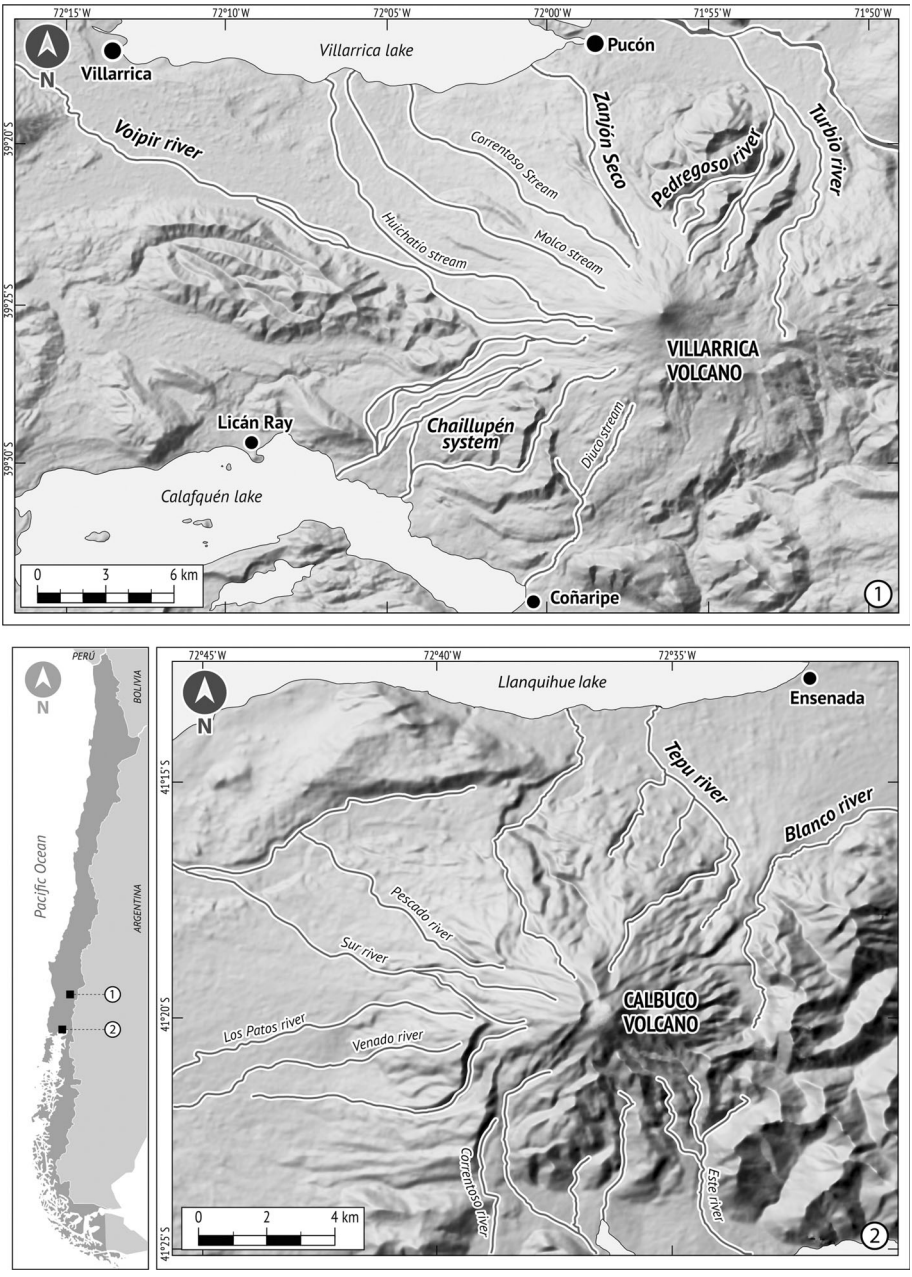

Fig. 1 Location map of Villarrica and Calbuco volcanoes. The main river systems and streams are indicated for each volcano

zones and creating confidence levels for each hazard zone. Despite the wide use of the programme, few authors have mentioned some of its limitations such as its strong dependence on DEM vertical accuracy, the output of unrealistic ragged inundation zones and the assumption of a fixed lahar volume.

In this paper, we apply the LAHARZ code to simulate lahar inundation zones around two of the most active volcanoes of the SVZ: Villarrica and Calbuco (Fig. 1). We chose these contrasting volcanoes because both have been very active in historical times. Also, each have good record of their eruptions during the last couple of centuries, and there are important populated areas in their surroundings. Both volcanoes have considerable snow cover in winter, and Villarrica also has glaciers. However, the lahars generated by the two volcanoes have had contrasting characteristics (Castruccio et al. 2010) in terms of their triggering and dynamic mechanisms.

We used LAHARZ to evaluate three factors that can affect the resulting outputs of the programme: (1) the influence of the DEM type, quality and vertical accuracy, using three different elevation datasets (i.e. SRTM, ASTER GDEM and a topographic map-derived DEM) to evaluate whether low-resolution but easily available DEMs are capable of simulating medium- to large-volume lahars; (2) the validity of one of the calibration constants used in the equations governing the global LAHARZ model when applied to lahars generated by two of the volcanoes in the SVZ; and (3) the influence of the changing topography during the emplacement of pulsed phases of lahars on the trajectory of subsequent flows.

2 Location and geological setting

2.1 Villarrica volcano (39°S)

Is the most active volcano of the SVZ with its summit located 20 km S of the town of Pucón. It has a large edifice built from Middle Pleistocene (ca. 600 ka) until present (Moreno and Clavero 2006). It has evolved in three main stages with the formation of at least two collapse calderas. The latest stage edifice (<3.7 ka) is comprised mainly by basaltic andesite lavas and deposits left by pyroclastic density currents, as well as abundant lahar deposits (Clavero and Moreno 2004). In historical times (i.e. within the last 500 years based on historical records), at least 60 eruptive events have been documented, most of them of hawaiian to mild strombolian type, although minor pyroclastic density currents have been observed (1948–1949 eruption) as well. The last eruptions that generated lahars occurred in 1948, 1963, 1964 and 1971. The 1964 eruption lahar destroyed the town of Coñaripe killing more than 20 people (Moreno and Clavero 2006). The volcano is covered by an ice cap with an estimated volume of 1.17 km^3 of water equivalent in 2012 (Rivera et al. 2014), as well as a seasonally changing snow pack. Lahars are mainly generated by the sudden melting of this ice/snow cover during eruptions, usually with lava fountains remobilizing loose material on the upper flanks of the volcano. Estimated individual historical lahar volumes are in the range of 5–50 $\times$ 10^6 m^3 (Castruccio et al. 2010) with estimated discharge rates in the order of 2–20 $\times$ 10^3 m^3/s (Naranjo and Moreno 2004).

2.2 Calbuco volcano (41°S)

Is an active volcano with its summit located $\sim$30 km NE of Puerto Montt city, one of the largest and economically most important cities in Southern Chile. Its evolution has been

characterized by the emission of lava flows and domes, mostly of silicic andesite composition, with associated pyroclastic flows and lahars (Lopez-Escobar et al. 1992; Sellés and Moreno 2011). The latter often are described as "hot" by Moreno and Naranjo (2004) and Moreno et al. (2006). The evolution of this volcano has also been marked by two sector collapses in the Holocene, with major debris avalanches directed to the west-northwest (Clavero et al. 2008). In historical times, Calbuco has had 11 eruptions, three of them corresponding to major eruptive cycles (1893–1895, 1929, 1961), with the emission of lava flows, ash fallout tephra and block-and-ash flows, with eruptive styles ranging from strombolian to subplinian (Petit-Breuilh 1999). There was a major eruptive event in 1893–1895. Lahars are generated at this volcano both by the sudden melting of ice/snow and by the dilution and mixing with water of block-and-ash flows. A minimum volume estimate for the 1961 lahar at the north flank was 5×10^6 m^3 (Castruccio et al. 2010), with an estimated discharge rate of 3×10^3 m^3/s (Klohn 1963).

3 Methodology

We used LAHARZ (Schilling 1998; Iverson et al. 1998) and the modified single flow (MSF) direction model (Huggel et al. 2003, 2007) algorithm to simulate the inundation areas associated to lahar flows of different volumes. LAHARZ has been widely applied to different volcanoes worldwide to generate hazard maps (e.g. Hubbard et al. 2007; Muñoz-Salinas et al. 2009; Huggel et al. 2007). It is a semi-empirical method that relates the total volume of the flow with the cross-sectional and planimetric areas of the resulting inundation zone.

The LAHARZ code uses two equations to calculate the cross-sectional and planimetric areas inundated by a lahar of a given value (Iverson et al. 1998):

$$A = K V^{2/3} \tag{1}$$

and

$$B = C V^{2/3} \tag{2}$$

where A and B are the planimetric and cross-sectional inundated areas, respectively, and V is the total volume of the lahar. The global model's calibration constants K and C (200 and 0.05, respectively) were based on data from past lahars, supplemented by experimental and non-volcanic debris flows.

Some of the limitations of the model include (1) the impossibility of the modelled flow to diverge into different paths; (2) underestimation of the spreading when encountering flat or unconfined terranes; and (3) no consideration of bulking and debulking processes (e.g. Vallance 2000). Another limitation of the LAHARZ approach to lahar hazard mapping is related to the fact that lahars usually develop in a number of individual waves rather than just one single pulse. Therefore, the flowage and deposition associated with several waves can modify the topography through erosion and deposition, changing the paths of later pulses. Finally, the calibration of the original global model was done considering different types of lahars (e.g. clay-rich and clay-poor—Vallance 2000) with very different volumes and flow characteristics from around the world. Therefore, the original calibration constants may not be adequate for lahars in certain areas with unique eruptive and emplacement characteristics.

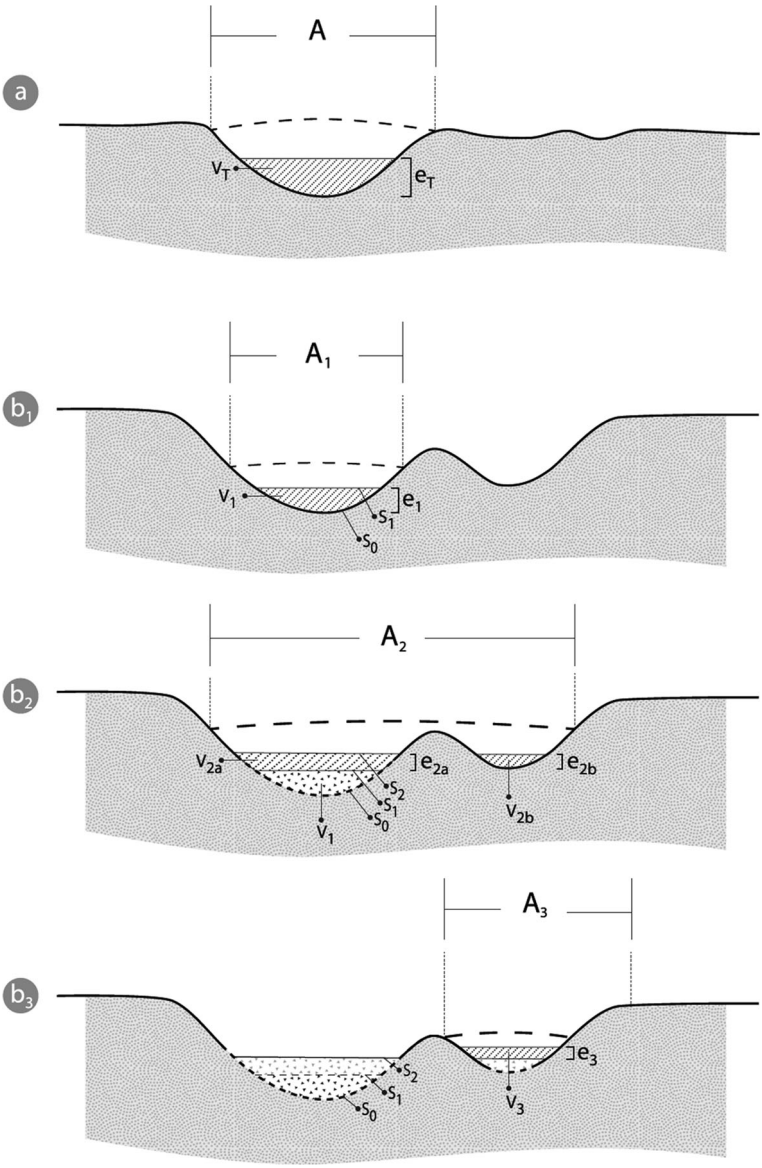

Fig. 2 Scheme with the variations of topography (shown on a cross section) that can be caused by a lahar and incorporated in the LAHARZ code. **a** A lahar flowing through a valley reaches an inundation level marked by the *dashed line*, covering a lateral distance A, but the resulting deposit (V_t) covers only a fraction of the inundated zone, reaching a thickness e_t, that typically is 1/3–1/5 of the inundation height. **b** Example of the variations on topography and the implications on lahar trajectories: $\mathbf{b_1}$ an initial wave inundates a sector marked by A_1. The resulting deposit is V_1, with a thickness e_1. The new surface is marked by S_1 (the previous surface was S_0). $\mathbf{b_2}$ A new laharic wave arrives (same volume), inundating an area marked by A_2. Because the left channel is shallower than before the inundation zone also affects the right channel, the deposit left is marked by V_{2a} and V_{2b}, with thicknesses e_{2a} and e_{2b}. The new surface is marked by S_2. $\mathbf{b_3}$ Because the left channel is almost filled with the deposits, the third wave flows exclusively over the right channel, inundating a zone marked by A3 (thus changing its trajectory) leaving the deposit marked by V_3

We attempted to fix some of these limitations in LAHARZ by firstly changing the calibration constant in order to re-calibrate the global model to better simulate the cross-sectional inundation patterns and thus run-outs of localized lahars from two volcanoes. Previous authors (Oramas Dorta et al. 2007; Widiwijayanti et al. 2009; Magirl et al. 2010) have changed the cross-sectional and planimetric constants of LAHARZ using different datasets to modify the model in order to better simulate the inundation areas generated by pyroclastic flows and non-volcanic debris flows. Oramas Dorta et al. (2007) changed the planimetric constant ($K = 200$) and the exponent (2/3) from Eq. (1), to adapt the model to non-volcanic debris flows in the South of Italy. They defined global and local models to indicate whether the relationship between total volume and planimetric area was obtained using data from different flows around the world (global) or only from the studied area (local). In this work, we only recalibrated the cross-sectional constant used by LAHARZ ($C = 0.05$ from Eq. 2) by reducing the dataset of Iverson et al. (1998) to cases with similar type and volume when compared with the lahars generated in the volcanoes of the Southern Andes, and adding data collected from Villarrica and Calbuco volcanoes. We did not attempt to carry out a rigorous mathematical procedure in order to derive a new calibration constant, but to test a different value adapted to the characteristics of Southern Andes lahars. It is important to note that by changing the cross-sectional constant, the inundated planimetric area and the run-out distance calculated by LAHARZ are also affected, as the cross-sectional widths obtained are different, thus changing the planimetric area per length unit.

We also generated new DEMs with the inundation zones generated by LAHARZ, to simulate subsequent flows with a modified topography due to deposition of previous waves (Fig. 2). As such, LAHARZ does not simulate deposits left by lahars, but rather inundation zones. In order to generate the new DEMs, we followed the relationship suggested by Quinteros (1991) where the thickness of the deposits left by a lahar at Llaima volcano, Southern Andes of Chile, is approximately 3–5 times lower than the maximum inundation depth or wave height. The code of LAHARZ was modified (see Appendix in ESM) in order to obtain a new DEM at the end of each run, adding the thickness of the inundated area generated by the programme. For example, if a lahar event is simulated as three pulses, LAHARZ should be run three times manually, each time using as input the new DEM generated in the previous run.

In order to compare the LAHARZ results with other flow models, we used the MSF code which was developed originally in glacial-derived flows (Huggel et al. 2003). The model was originally implemented to simulate glacier lake outbursts (Huggel et al. 2003) and has later been applied to lahars on the Popocatépetl volcano (Huggel et al. 2007). In general terms, the MSF code allows to better estimate the lateral extension of the inundation probability by lahars than the LAHARZ code as it has implemented a special function to determine the flow paths that reproduces better the distribution of the flow in flatter terrains. The run-out distances predicted by the MSF model are less reliable though as they are calculated beforehand by choosing a fixed H/L value, where H is the height drop and L is the horizontal distance. The flow stops when the critical H/L is finally reached. Lahar flows have a high mobility, and attempts to model their run-out distance by choosing an H/L value has proven inadequate (Huggel et al. 2007). The MSF model is integrated in the ARCGIS suite and estimates the "cost" or probability of a DEM cell to be inundated as a function of the distance from the origin and the distance from the steepest path (for more details, see Huggel et al. 2003).

3.1 DEMs used

We used three different DEMs to simulate the lahars at Villarrica and Calbuco volcanoes. The SRTM, ASTER GDEM and a DEM generated from the contour intervals from topographic maps at 1/50,000 scale, with contours intervals every 50 or 25 m generated by

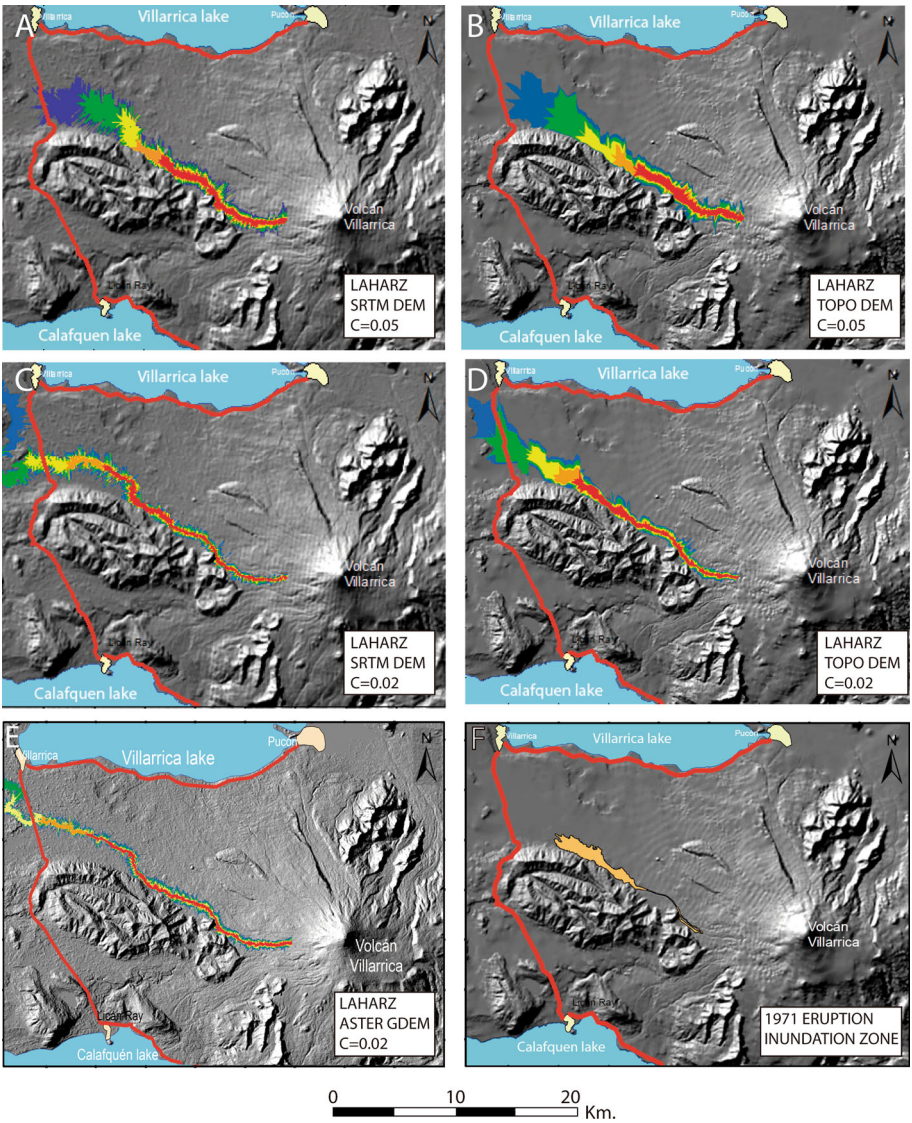

Fig. 3 LAHARZ simulations on the Voipir river (Villarrica volcano) using volumes of 100 (*blue*), 50 (*green*), 20 (*yellow*), 10 (*orange*) and 5 (*red*) x10^6 m^3. **a** Original LAHARZ using the SRTM DEM. **b** Original LAHARZ using the topographic DEM. **c** LAHARZ with c = 0.02 (see text) and SRTM DEM. **d** LAHARZ with c = 0.02 and topographic DEM. **e** LAHARZ with c = 0.02 and ASTER GDEM. **f** Deposits left by the 1971 lahar (estimated volume of 20 × 10^6 m^3). *Red lines* are main roads

the Instituto Geografico Militar (IGM) of Chile. The SRTM DEM was developed by the NASA in 2000 and has a horizontal resolution of 90 m for areas outside of the continental USA and its overseas territories. The data were obtained from http://srtm.csi.cgiar.org where the original data were processed to fix errors in zones with very high slopes or water bodies. The ASTER GDEM was developed in 2009 by the NASA and the Ministry of Economy, Trade and industry of Japan. Version 2 of ASTER GDEM was released in 2011

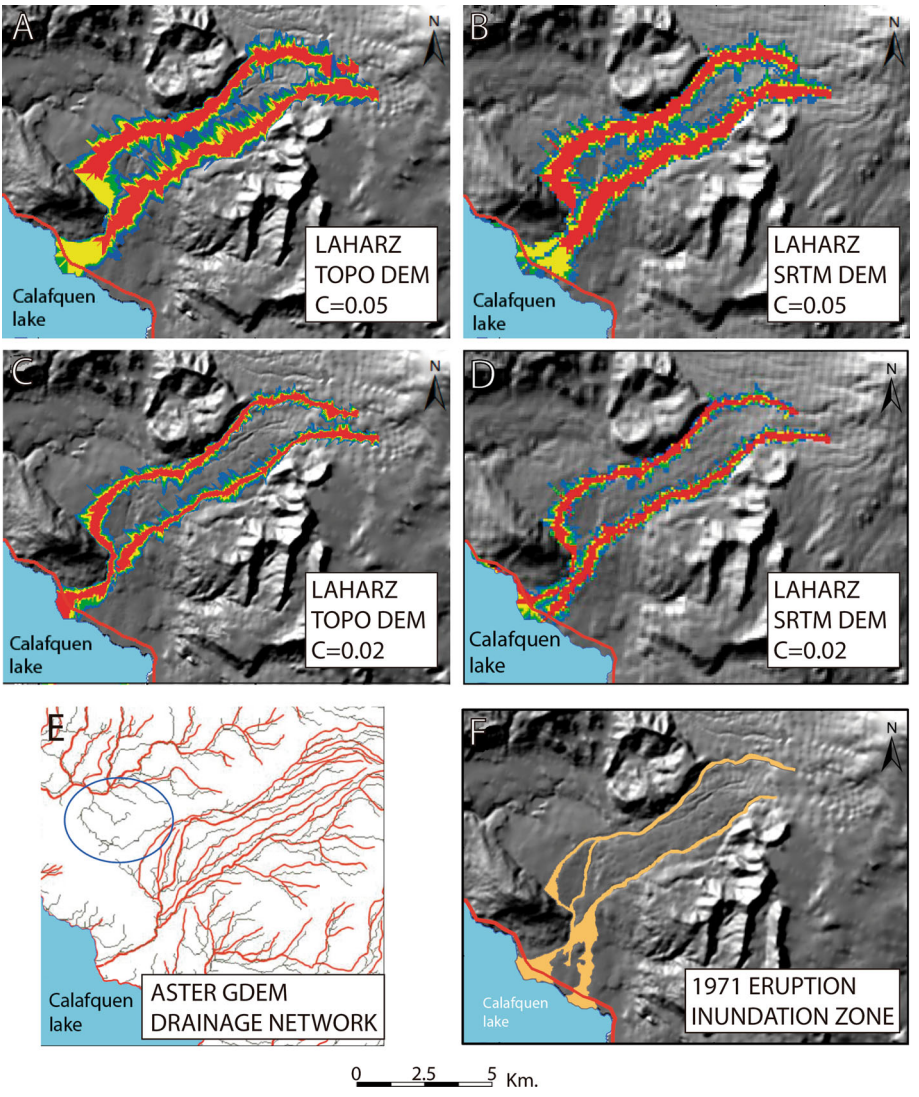

Fig. 4 LAHARZ simulations on the Chaillupen system (Villarrica volcano) using volumes of 50 (*Blue*), 20 (*green*), 10 (*yellow*) and 5 (*red*) $\times$ 10^6 m^3. **a** Original LAHARZ using the topographic DEM. **b** Original LAHARZ using the SRTM DEM. **c** LAHARZ with c = 0.02 (see text) and topographic DEM. **d** LAHARZ with c = 0.02 and SRTM DEM. **e** Stream trajectories identified in the ASTER GDEM (*black lines*) compared with the real ones (*red*). There are big discrepancies that are indicated by the *circle*. **f** Deposits left by the 1971 lahar (estimated volume of 10 $\times$ 10^6 m^3)

with improvements in accuracy and resolution and reduced presence of artefacts. The data were obtained from http://gdem.ersdac.jspacesystems.or.jp/. The ASTER GDEM was only tested at Villarrica volcano. The main source of inaccuracies in both SRTM and ASTER GDEM is due to the canopy cover, which could be taken erroneously as the topographic surface in zones with dense vegetation, making channels appear deeper than they really are (e.g. Hubbard et al. 2007).

4 Results

4.1 Villarrica volcano

We tested the original LAHARZ code in the Voipir and Chaillupen streams at Villarrica volcano, where detailed sedimentological and textural analyses were carried out on the 1971 lahar deposits (Castruccio et al. 2010). The range of volumes was chosen for each case according to estimates based on volumes of lahars from past eruptions (Naranjo and Moreno 2004; Castruccio et al. 2010) and available water equivalent from glaciers and snow (Moreno 1993; Brock et al. 2007; Rivera et al. 2014). We chose volumes of 100, 50, 20, 10 and 5 $\times$ 10^6 m^3 in the Voipir river and 50, 20, 10 and 5 $\times$ 10^6 m^3 in the Chaillupen case (Figs. 3, 4, respectively. For comparison, we also included in Figs. 3f, 4f the deposits left by lahars during the last eruption in 1971). Figure 3a, b shows the results with the SRTM and topographic DEMs in the Voipir river. In both cases, there is no clear distinction between channelized and open-plain overflow areas, regardless of the initial flow volume used. The results also show that the cross-sectional extents of the simulated inundation zones are overestimated. Consequently, the run-out distances are subestimated when compared with field observations and previous geological and hazard maps (Moreno 2000; Moreno and Clavero 2006). For example, the 1971 lahar had an estimated volume of 2 $\times$ 10^7 m^3 approx. (assuming a water content of $\sim$50 % by vol.; Pierson et al. 1990; Vallance 2000) and reached 24 km from the summit of the volcano, while the simulations with the same volume only reached 20 km. Even for the largest simulated flows (10^8 m^3), the run-out distances obtained are <30 km from the summit, while lahars of such magnitude form previous eruptions (1640, 1948–1949; Moreno and Clavero 2006) reached the Tolten river, more than 40 km from the summit.

The results with the SRTM and topographic DEMs in the Chaillupen stream are shown in Fig. 4a, b. The inundation zones are similar to the results in the Voipir river, with cross-sectional extents that are exaggerated when compared with previous lahars (Fig. 4f) and shorter run-out distances than historical flows (Fig. 4a, b). For example, a simulation of a 5 $\times$ 10^6 m^3 flow does not reach the Calafquen Lake, while all historical lahars of this magnitude have reached the lake.

The simulations based on the ASTER-derived DEM result in very restricted or confined lateral extensions (Fig. 3e) without a good discrimination between the channelized flows and inundation zones that overbank into neighbouring drainage channels. In the Chaillupen stream, the calculated stream trajectories could be different from the real ones, and consequently the simulations would give unrealistic results (Fig. 4e). We attribute these problems to the dense forest canopy and smooth underlying topography of the bald earth surface, with shallow (<15 m) channel wall depths in most streams.

Table 1 Selected data used to re-calculate the transversal area constant used in Eq. (2)

Volcano	River	Volume (10^6) (m^3)	Discharge (m^3/s)	Transversal section (m^2)	mean velocity (m/s)	Constant (Eq. 2)	Source
Mount Hood	ZigZag	73	–	12,000	–	0.0687	Iverson et al. (1998)
Nevado del Ruiz	Azufrado	40	–	2,300	–	0.0197	Iverson et al. (1998)
Nevado del Ruiz	Molinos Nereidas	30	–	1,100	–	0.0114	Iverson et al. (1998)
Nevado del Ruiz	Guali	16	–	2,000	–	0.0315	Iverson et al. (1998)
St. Helens	Pine Creek + Muddy River	14	–	2,100	–	0.0361	Iverson et al. (1998)
	South Fork Toutle	12	–	1,500	–	0.0286	Iverson et al. (1998)
Mayon	Mabinit	1.2	–	200	–	0.0177	Iverson et al. (1998)
					Mean value	0.0305	
Villarrica	Correntoso	33	10,000	1,000	10	0.0097	Naranjo and Moreno (2004)
Villarrica	Pedregoso	42	12,000	2,400	5	0.0198	Naranjo and Moreno (2004)
Villarrica	Turbio + Pedregoso	80	20,000	2,000	>10	0.0107	Naranjo and Moreno (2004)
Villarrica	Chaillupén	33	10,000	1,000	10–14	0.0097	Naranjo and Moreno (2004)
Villarrica	Coñaripe	17	6,000	750	>10	0.0113	Naranjo and Moreno (2004)
Villarrica	Voipir	20		1,500		0.0203	This study
Calbuco	Tepú	10		600		0.0129	This study
Calbuco	Tepú	7.2	3,000	545	6	0.0146	Klohn (1963)
					Mean value	0.0136	

4.1.1 Cross-sectional constant calibration

We tested whether the choosing of a different calibration constant for localized calculation of the cross-sectional area (Eq. 2) could give a better fit of the results when compared with published hazard maps and/or the record of past eruptions deposits. In this case, we estimated the cross-sectional area and total volume for some lahars from Villarrica and Calbuco volcanoes (Table 1), and we also included data from lahars with similar volumes from Iverson et al. (1998). From this new dataset, based on lahar flows more similar rheologically to those usually generated in the SVZ, we chose a constant of 0.02 instead of the original 0.05 (by changing this value in the make_lahar.aml script of the LAHARZ suite, see Appendix in ESM) to test whether the results are more in accordance with the field observations and calculations of the lahars of Villarrica and Calbuco volcanoes. It is worth stating that due to the few data available, we did not attempt to calculate a new value in a mathematically rigorous way (e.g. Oramas Dorta et al. 2007), but rather test whether a different value could give a better result for lahars of this zone.

Figure 3c, d shows the results of the modified LAHARZ using the new constant in the Voipir river at Villarrica. It is very clear that the cross-sectional extent of the inundation areas is more restricted and much closer to field observations and that the run-out distances

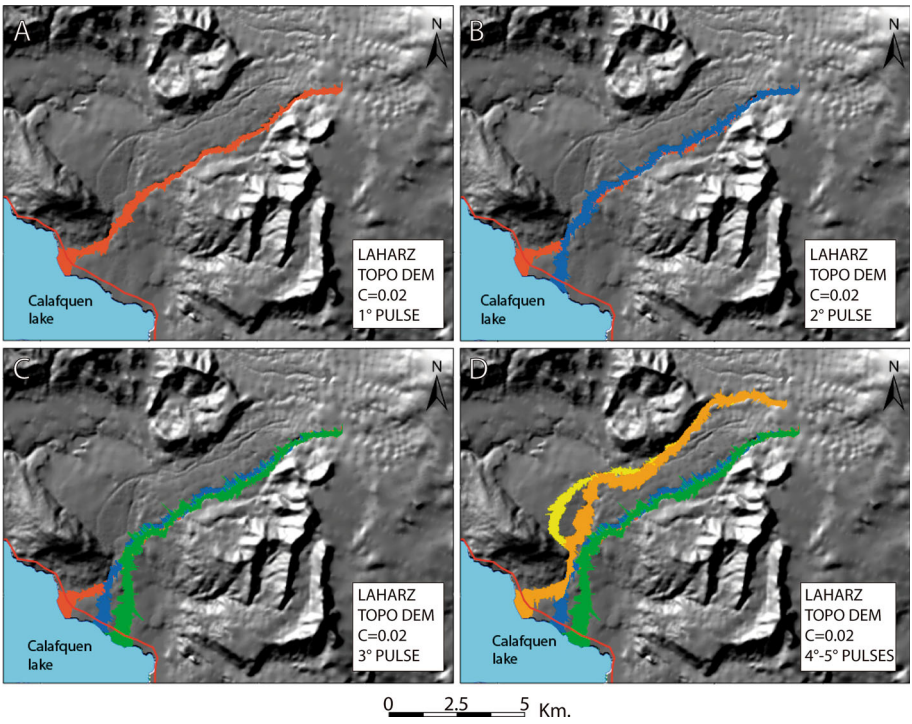

Fig. 5 LAHARZ simulations on the Chaillupen system in which each simulation changes the topography for the next pulse (using recalibrated cross-sectional constant c = 0.02). **a** First pulse (5×10^6 m^3). **b** Second pulse (in *blue*) with the same volume. **c** Third wave (*green*). Same volume of 5×10^6 m^3. **d** Fourth and fifth pulses (*yellow* and *orange*) in the N branch of the system

are better matched with historical events. The same better fit is observed in the Chaillupen stream (Fig. 4c, d).

The results with the topographic DEM in the Voipir river are the closest to the historical lahar inundation zones. The topographic DEM is also the DEM that best differentiate between channelized and overflow areas (Fig. 3d). Both the SRTM and ASTER GDEMs are more restricted in their lateral extent areas and do not resolve correctly the overflow zones (Fig. 3c, e). In the Chaillupen stream, there are no significant differences between the results obtained with the SRTM and the topographic DEM, both in terms of cross-sectional width and run-out distances (Fig. 4c, d). The ASTER GDEM was not tested in this case because important errors were detected in the stream paths (Fig. 4e). Similar errors were detected by Stevens et al. (2002) at Ruapehu and Taranaki volcanoes in New Zealand, and Hubbard et al. (2007) at Citlaltepetl volcano in Mexico.

4.1.2 Changes in topography

We also tested the influence of a changing topography over the modelled inundation zones as a consequence of deposition of previous laharic pulses during a single eruptive cycle, as has been described for historical cases at Villarrica volcano (Naranjo and Moreno 2004). The code was modified in order to generate a new DEM after the occurrence and deposition of each individual pulse, by adding the estimated deposited material using the LAHARZ modelled inundation zones. As LAHARZ simulates inundation zones and not the resulting deposits, we approximated the deposit thicknesses as 1/3 of the inundation zone cross-sectional area (Fig. 2), based on our field observations and data from Quinteros

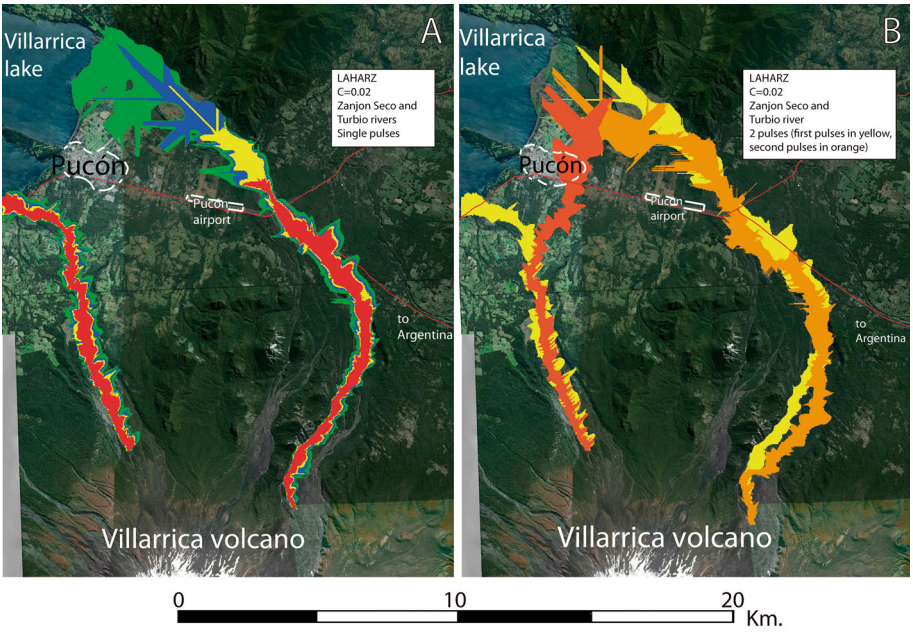

Fig. 6 LAHARZ simulation on the Tepu river (Calbuco volcano) as three consecutives waves of 5×10^6 m^3 each (using recalibrated cross-sectional constant c = 0.02). **a** First wave (*red*). **b** Second wave (*green*). **c** Third wave (*orange*). **d** Deposits left by the 1961 lahar (minimum estimated volume of 5×10^6 m^3)

(1991) obtained at the neighbour Llaima volcano. Although we are aware that this corresponds to a rough approximation as the relationship between maximum inundation level and deposit thickness depends on several factors such as flow velocity, slope, solid concentration, topography, etc., our aim is to explore and test improvements on the LAHARZ code rather than to simulate exactly the inundation areas of historical events. The 1/3 value

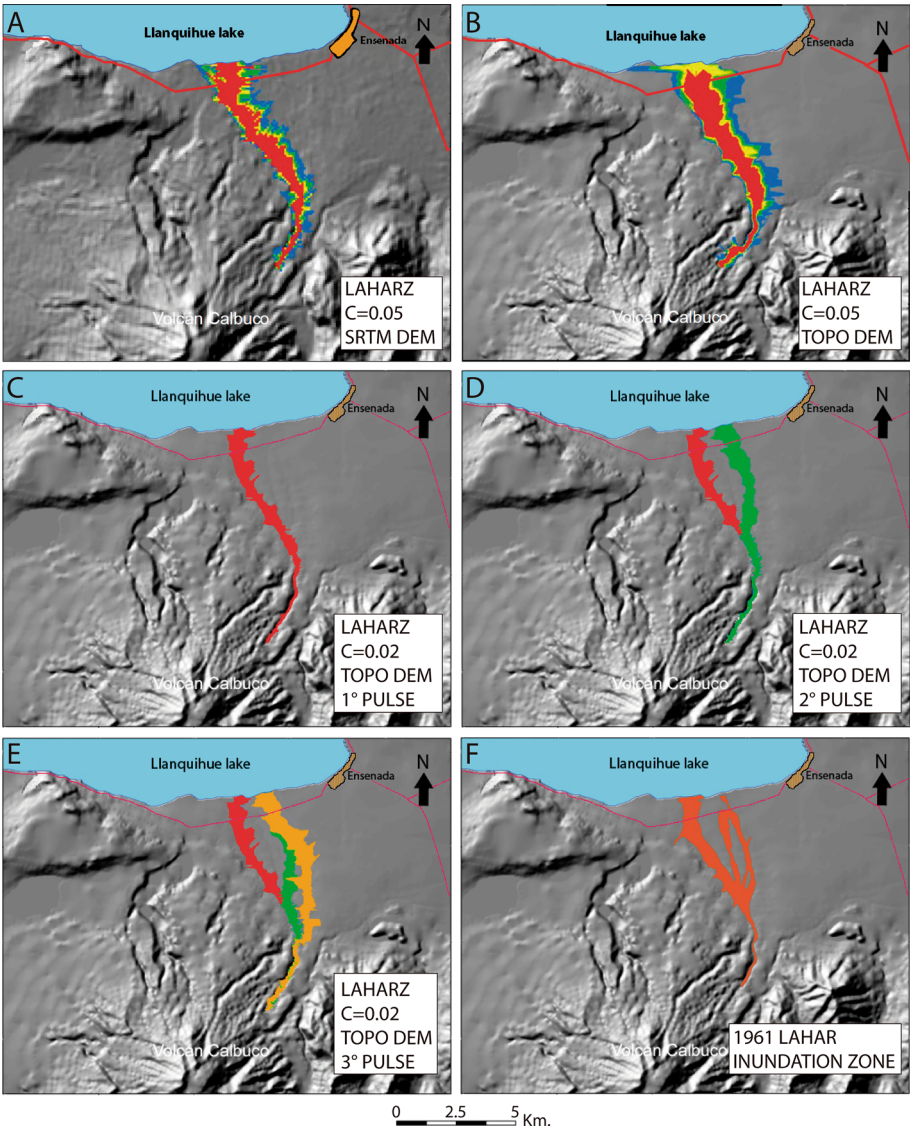

Fig. 7 LAHARZ simulations on the Zanjón Seco and Turbio rivers, N flank of the Villarrica volcano (using recalibrated cross-sectional constant c = 0.02). *Solid line* indicates the Pucón town, *dashed line* indicates the urban limit. **a** Simulations with 50, 20, 10 and 5 × 10^6 m^3 in the Zanjón Seco and 100, 50, 20 and 10 × 10^6 m^3 in the Turbio river. **b** Simulation of lahars as two consecutive waves of 20 × 10^6 m^3 in the Zanjón Seco river and of 50 × 10^6 m^3 in the Turbio river

used here between flow heights and the resulting lahar deposits seems reasonable. The modifications to the code are shown in the Appendix in ESM.

Figure 5 shows the results of the modifications of the LAHARZ code when applied to the Chaillupen stream. We simulated a lahar event as five pulses of 5×10^6 m^3 over the two main channels where the lahars of the 1971 eruption flowed. Figure 5a–c shows the results with three pulses over the S channel and Fig. 5d shows the results with two pulses over the N channel. Each of the three pulses over the S channel followed the same path over the channelized section, but once they reach more open-plain areas, closer to the lake shoreline, the pulses diverge, with every subsequent flow going further to the SE than the previous one. The second pulse in the northern channel followed the same path than the first one with the exception of a part in the middle section where it followed a secondary channel for a couple of kilometres before returning to the main channel. The total inundated area followed by the five pulses cover a larger area than the original LAHARZ results. More importantly, the resulting paths are more similar to the paths followed by the 1971 lahars.

The importance of topographic changes due to deposition in hazard assessment can be clearly observed in the Zanjón Seco and Turbio river cases, on the northern flank of the Villarrica volcano (Figs. 1, 6) near the town of Pucón. In this case, the results of the original unmodified LAHARZ, using volumes of 5, 10, 20 and 50×10^6 m^3 did not reach the town. Even for the largest volumes, the lahar paths only reach areas to the south and north of Pucón (Fig. 6a). However, when we simulated a single lahar event as being formed by a series of individual discrete pulses over an evolving topography, the results were very different. We simulated a lahar of 2×10^7 m^3 as two consecutive pulses, each of 10^7 m^3 in both rivers. In the Zanjón Seco case (Fig. 7b), the first wave of 10^7 m^3 follows the same trajectory of the unmodified code, but the second wave deviates 5 km before reaching the Villarrica Lake shoreline and diverts following a NNE direction, reaching and inundating more than 50 % of the town of Pucón's area. The total inundated area is greater than the single-pulse 20×10^6 m^3 lahar, with 3.5 km^2 of new inundated zones to the East of the main channel. Our results are also more in accordance with the delineated hazard zones for the official hazard map of the Villarrica volcano constructed by Moreno (2000) based on the observations of the deposits left by past eruptions (Moreno and Clavero 2006). A similar situation arises in the Turbio river case. Here, we simulated a 50×10^6 m^3 lahar as two discrete pulses of 25×10^6 m^3. In this case, the results are similar to the Zanjón Seco simulations, with an increased inundated area, affecting the northern outskirts of Pucón, which were not affected when the lahars were simulated as a single pulse.

4.2 Calbuco volcano

LAHARZ simulations on the Calbuco volcano (Tepu River, northern flank of the volcano) are shown in Fig. 7. The results with the unmodified code using the SRTM and topographic DEMs (Fig. 7a, b) also show very wide cross-sectional areas that are larger than inundated areas of past events (Fig. 7f shows the extent of the 1961 event, with an estimated volume of 10^7 m^3). To test the effects of the changes made to LAHARZ in this river, we simulated a 15×10^6 m^3 lahar flow divided into three individual pulses of 5×10^6 m^3 with the modified cross-sectional constant set to 0.02. The results (Fig. 7c–e) show that all the pulses followed the same path over the channelized zone, but once they reach a smoother open-plain topography, the pulses begin to diverge, following different paths, each time further to the East. The resulting inundation areas for the three pulses cover an area which

is more similar to the area inundated by the 1961 lahars than the original simulations with the unmodified LAHARZ (Fig. 7d).

4.3 MSF code simulations

For comparison, we applied the MSF code to some of the streams simulated using LAHARZ at Villarrica and Calbuco volcanoes (Figs. 8, 9, 10).

4.3.1 Villarrica volcano

Figure 8 shows the results of the MSF model in the Voipir river system using the Topography-derived and SRTM DEMs. Important differences are observed in the modelled inundation zones probabilities. The channelized and overflow sections can be clearly

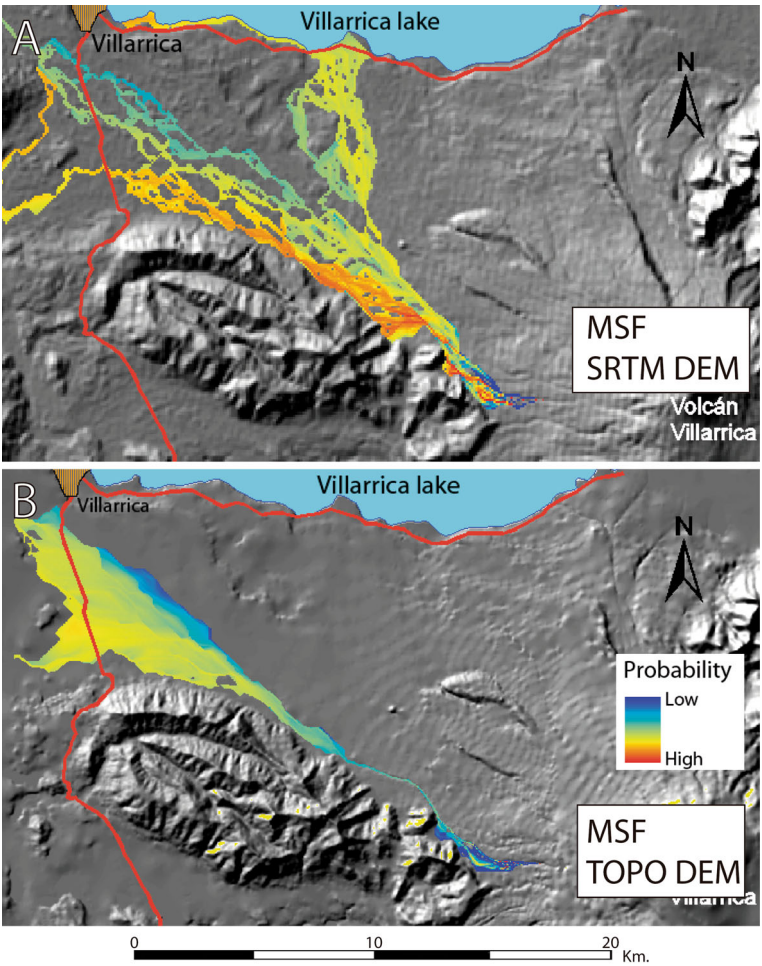

Fig. 8 MSF simulations on the Voipir river with **a** SRTM DEM and **b** topographic DEM. *Colours* indicate the relative probability of an area of being inundated

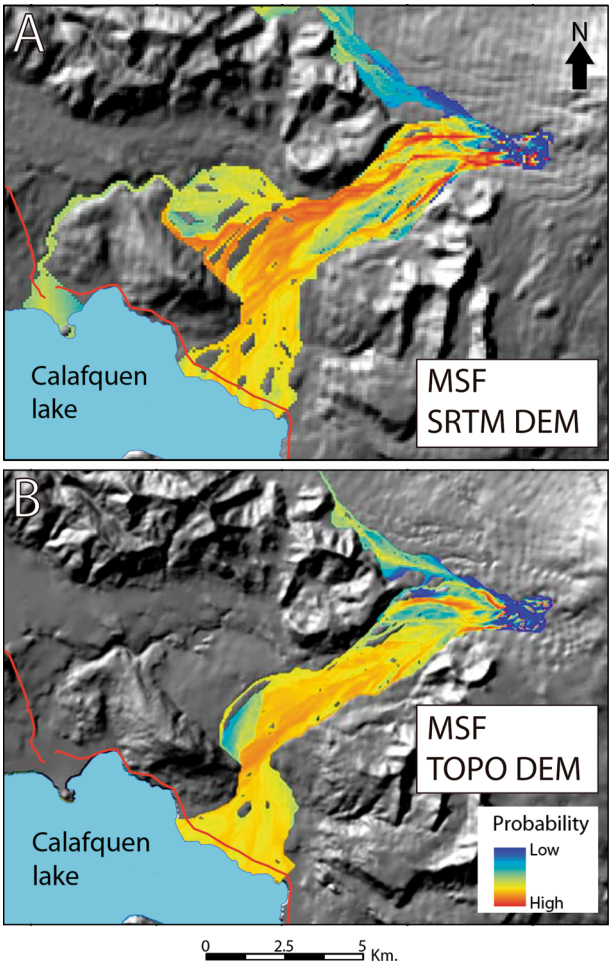

Fig. 9 MSF simulations on the Chaillupen system with **a** SRTM DEM and **b** topographic DEM. *Colours* indicate the relative probability of an area of being inundated

identified on the topographically derived DEM, and the planimetric shape up to 20 km from the crater is similar to the limits of the deposits of past eruptions. After this distance, the inundated areas cover a broader area laterally, but the zones with highest probability follow the actual channel of the Voipir river. The results with the SRTM DEM are more complex with the flow diverging into different streams as in the Huichatio River that reaches the Villarrica Lake towards N. The channelized zone is not clearly identified as in the topographic DEM, but the highest probability zones roughly coincide with it.

At the Chaillupen system, the results using both the SRTM and topographic DEMs are very similar to each other, with the exception of the W side of the inundation zone (Fig. 9). The inundation zone in this sector is very confined when using the topographic DEM, but in the SRTM simulations, this zone is bigger and a small branch reaches the Calafquen lake, affecting the town of Lican Ray, although with a low relative probability. In the

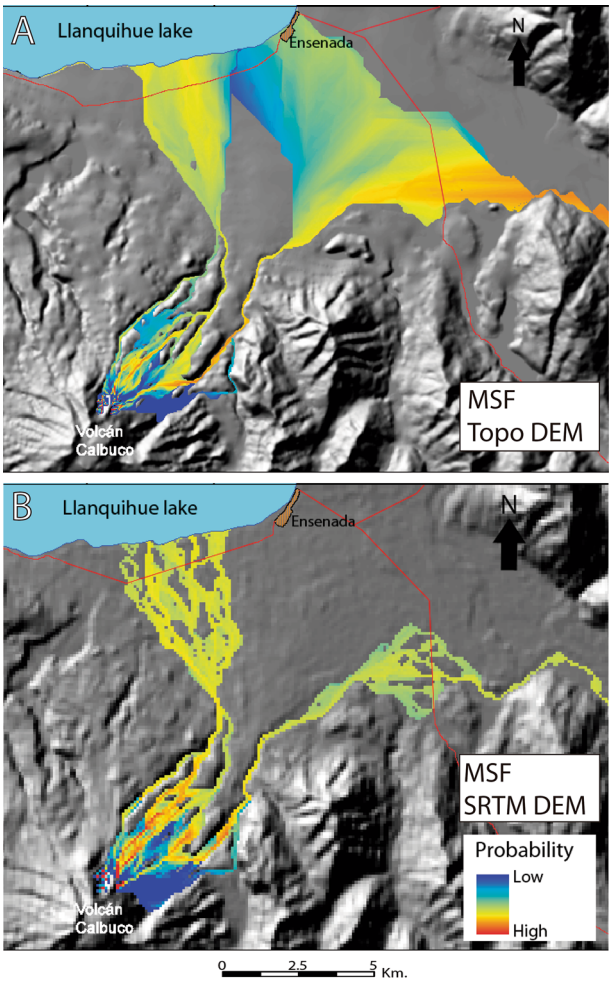

Fig. 10 MSF simulations on the Tepu river with **a** SRTM DEM and **b** topographic DEM. *Colours* indicate the relative probability of an area of being inundated

hazard map of Moreno (2000), this zone is recognized as prone to be affected by lahars, but no historical lahars have followed this path.

4.3.2 Calbuco volcano

The results obtained with the SRTM and topographic DEMs in the Tepu river (Calbuco volcano) are very similar to each other and cover roughly the same areas (Fig. 10). A notable discrepancy is observed to the N of the HueñuHueñu river, where a much bigger inundation area is obtained when using the topographic DEM. However, the zones with highest inundation probability are equivalent. The discrepancies are probably reflecting the spacing of the contour lines that generated the topographic DEM, as the area involved is very flat.

5 Discussion

5.1 DEM Comparison

From the results presented in the previous section, it is clear that the ASTER GDEM has some problems when it is used for simulating lahar inundation zones. The resulting inundation zones have narrow cross-sectional areas, even in very flat areas where overflow occurs. Additionally, in some areas, the paths obtained are not realistic as they follow different trajectories compared to the actual hydrology of the area. These problems result from areas with dense vegetation. The study area is densely forest covered with canopy tops that are wrongly identified as topographic surfaces during the generation of the DEM from the ASTER stereo pair images. This effect also appears in the SRTM DEM but is less marked. These problems have also been previously reported by diverse authors (Stevens et al. 2002; Hubbard et al. 2007; Huggel et al. 2007). In the case of the Villarrica and Calbuco volcanoes, this issue is probably more serious than in the previously reported cases due to the smoother topography of the valleys surrounding these SVZ volcanoes than the other volcanoes studied in Mexico and New Zealand by others authors. At Villarrica and Calbuco, the channel walls in the cross-channel zones are generally <10 m deep, and consequently the vegetation heights are comparable. The SRTM and topographic DEMs reproduce much better the inundation zones, but with noticeable differences. The topographic DEM mimics better the transition from more channelized to open-plain zones, as can be clearly seen in the Voipir river (Figs. 3, 8). This is probably due to the better horizontal resolution of the topographic DEM (30 m) compared with the SRTM (90 m) as some of the channels are very narrow (<50 m). On the other hand, the results obtained with the SRTM seem to better identify the different paths that a lahar can follow as shown in the Chaillupen stream where a secondary channel that reaches the town of Lican Ray was detected by the MSF code as a possible lahar path (Fig. 9). Other authors (Stevens et al. 2002; Hubbard et al. 2007; Huggel et al. 2007), however, have reported little differences between the results using different DEMs. Thus, our result discrepancies between the different DEMs are probably due to the low relief of topographic features in the study areas, where channel walls are usually <10 m deep in channelized sectors and <5 m deep in open-plain sectors, which are very small when compared with the topography surrounding other volcanoes, where small differences in elevation between DEMs are less important for the flow simulations because the channels are usually much deeper (i.e. >50 m).

Our results indicate that despite the low spatial resolution of the DEMs used, it is still possible to simulate medium- to large-volume lahars using them. The lateral and longitudinal extents of the simulations compare well with estimations of previous eruptions (Moreno and Clavero 2006; Castruccio et al. 2010), and the MSF code differentiates channelized areas from open-plain areas better. Consequently, during an eruptive crisis, it is possible to use easily available and inexpensive low-resolution DEMs to rapidly evaluate the hazards associated with lahars at these volcanoes and make decisions.

5.2 Modifications to the LAHARZ code

Our results indicate that the simulations made using a cross-sectional area to volume model calibration constant of 0.02 (instead of the original 0.05) yield much better maps of likely lahar inundated areas at both volcanoes, when compared to those produced during historical events (Moreno 1999, 2000). We chose this constant according to the following

criteria: (1) actual measurements of the cross-sectional inundation areas covered by some historical lahars at both volcanoes; (2) use of published data for Villarrica volcano (Naranjo and Moreno 2004); and (3) inclusion of data from the original lahar volume versus cross-sectional area dataset used to calibrate LAHARZ (Iverson et al. 1998), but selecting lahars with similar volume (10^6–10^8 m^3) and character (non-cohesive). It is clear from our results that the selection of an appropriate constant is critical for an adequate hazard evaluation, as not only the lateral distribution is affected but also the run-out distance. The results obtained from our simulations after changing the constant show narrower inundated zones and longer run-outs compared to the results using the calibration constant of the original global LAHARZ model.

Consequently, before the application of LAHARZ to simulate lahar inundation zones on a specific volcano at a specific geotectonic location, it is necessary to determine the most likely type of lahar that will be generated by the volcano. Also necessary is a priori knowledge of the range of volumes that can occur during an eruption in order to derive a more appropriate calibration constant, in case local and historic conditions at the volcano being modelled differs from those of the global dataset used to calibrate LAHARZ in the first place (i.e. Iverson et al. 1998). It is also important to mention that we did not attempt to re-calculate a local model for the planimetric area constant (e.g. Oramas Dorta et al. 2007). For the two volcanoes studied in this work, it is very difficult to estimate planimetric areas of past lahars, because most of these flows reached lake shorelines before they stopped. It would be useful to estimate a local planimetric constant with data from other volcanoes of the SVZ to obtain a more complete recalibration of LAHARZ to adapt the model to the conditions of the SVZ.

Experimental work on debris flows (Major 1997) and studies on changes on the drainage after an eruption (Renschler 2005) confirm the importance of topographic changes to the flow paths of subsequent lahars. These changes can even occur during a single eruptive event, as lahars typically develops in different waves or pulses (Pierson et al. 1990; Iverson 1997; Naranjo and Moreno 2004). The occurrence of multiple waves has been observed in the deposits of the Villarrica and Calbuco lahars from 1971 to 1961 eruptions, respectively (Castruccio et al. 2010). Our results highlight the importance of doing simulations by dividing lahar events into a series of pulses or waves, which changes the topography after deposition of each pulse and, therefore affects the flow trajectory of the following wave. This fact can be observed from the results obtained with the LAHARZ code at Villarrica and Calbuco volcanoes (Figs. 5, 6, 7). The areas covered by simulations using changing topographic DEMs are much larger in certain rivers. In some cases, (e.g. Zanjón Seco and Turbio rivers, Villarrica volcano) the differences between runs with or without changes to the topography are critical for hazard evaluation of some areas, such as Pucón. The results show that when using a changing topography due to the deposition of previous pulses during the passage of a lahar, large parts of the town of Pucón are inundated as has happened historically (Moreno 2000; Moreno and Clavero 2006). The area covered at both volcanoes using topographic changes in between successive wave pulses are also closer to both the deposits left by past eruptions, as well as the hazard zones delineated on the official volcano hazard maps constructed using other empirical methods by Moreno (1999, 2000). Although our results using topographic changes seem promising and match in a better way the real data from last eruptions, they should be accepted with some caution. Firstly, we assumed that the observed deposits in the field correspond to $\sim 1/3$ of the maximum inundation level based on field observations (e.g. Quinteros 1991; Naranjo and Moreno 2004). However, this is not always the case, and the patterns of deposition/erosion can be very complex on the local scale. Secondly, our results were

obtained using DEMs that were generated after the last eruptions in both volcanoes. Thus, a comparison of our results with previous eruptions is not straightforward as the topography has changed. Nevertheless, our results seem to better simulate the multiple trajectories followed by most of the historical lahars at these volcanoes (Naranjo and Moreno 2004; Castruccio et al. 2010) that the original LAHARZ code is unable to do. Another limitation is that freshly generated deposits sometimes are non-cohesive and therefore can be easily eroded by new flows, something that is not possible to introduce to the LAHARZ code or DEMs used as inputs. This means that for extremely loose lahar deposits, the subsequent waves could easily erode the previous deposits in a manner that is not possible to model. Therefore, the inundation areas obtained for subsequent pulse waves may not be modelled correctly.

Our observations of the local characteristics of the studied volcanoes, modifications to LAHARZ, and subsequent results of re-calibrating to these local conditions, reinforce the need for field data prior to the use of software for hazard evaluation purposes. The critical parameters that should be measured or compiled from past studies are: (1) the volumes of past lahars and (2) the character of the flows (cohesive vs. non-cohesive) in order to choose the correct calibration constant (s) if either recalibrating the global model or deriving new scaling factors for a local model (e.g. Oramas Dorta et al. 2007). It is also important to check the occurrence of multiple waves or pulses during past lahar events. Even a single lahar event can be modelled as different pulses in order to identify secondary streams that could become inundated by later lahar trajectories that otherwise may not be identified.

5.3 Comparison between flow models

As mentioned by Huggel et al. (2007), a direct comparison between LAHARZ and MSF is difficult because while LAHARZ simulates inundation areas as a function of volume, MSF gives the probability of every cell being inundated from a flow generated from a certain cell or area of given steepness. The main advantage of MSF over LAHARZ is the former's ability to simulate the bifurcation of a flow to different paths. This is especially important in low-slope open-plain and complex topography, which is the case for instance of the Chaillupen stream. In such cases, the inundation areas obtained by MSF are more realistic when compared with historical lahars (Moreno 1999, 2000), and include stream trajectories not used by LAHARZ for streams that reach the town of Lican Ray on the SW flank of the Villarrica volcano (Fig. 9). Another advantage of the MSF code is its better discrimination between channelized flows versus overbank or unconfined flow zones, a fact that for lahars that can be observed in the Voipir river (Fig. 8). On the other hand, the LAHARZ code better determines lahar run-out distances, especially since the MSF code uses a single H/L coefficient which is better suited for debris avalanches and pyroclastic flows (e.g. Malin and Sheridan 1982). Another advantage of the LAHARZ code is that it gives run-out distances as a function of flow volume, allowing for the simulation of different eruptive scenarios.

6 Conclusions

Our results indicate that default cross-sectional calibration constant used by the global LAHARZ model is not appropriate for lahars generated at SVZ volcanoes. We revaluated this parameter in order to obtain results more consistent with historical lahars produced by this active volcanic range, in order to improve current hazard maps. Our results indicate

that a value of $C = 0.02$ for the calibration constant is more appropriate for lahars generated at Villarrica and Calbuco volcanoes.

One of the main results of our study is the relevance that a changing topography has on flow trajectory during lahar events formed by several pulses. Simulating multi-pulse lahars, in which each pulse modifies the topography due to the deposition of material, correlates much better with field deposits and the emplacement styles of historical lahars, as illustrated on published hazard maps constructed using empirical methods. This indicates that lahars can sometimes follow completely different trajectories if topographic changes occur due to the sedimentation of previous waves, even during a single eruptive event without much time between the successive wave pulses.

The MSF model is able to better simulate the cross-valley extent of lahars, by identifying both the confined/channelized and unconfined/plain zones in a better way than the LAHARZ code does. The MSF code is also better suited for delineating individual flow trajectories, since they are not limited to the steepest slope. This implies that the differences observed between lahar deposits and those simulated by LAHARZ could be due to the method used to calculate the inundation zone, rather than the DEM accuracy. Among the DEMs used, the DEM obtained from topographic contour lines (1:50,000) appears to give the best results, with the exception of flat plain areas where the contour lines are widely spaced (i.e. 50 m) and interpolation of elevation values are less precise. The ASTER DEM seems to be vertically the least accurate, due to the very dense forest canopy of this zone. This makes the simulation unrealistic, with consistently narrow inundation zones, even in plain areas. This problem is also apparent in the SRTM, although to a lesser extent. The biggest differences between the SRTM and topographic contour-derived DEMs are evident in the plain zones, where the SRTM seems to simulate better the high-hazard zones, while the topographic DEM sometimes over- or underestimate the inundation zones.

Our results indicate that it is possible to run lahar simulations of medium-to-large volume flows using low-resolution DEMs with both LAHARZ and MSF codes. This is especially important in areas with a high probability of lahar occurrence where there is no availability of high-resolution DEMs during a volcanic crisis, as in several volcanoes of the SVZ of Southern Chile. Such models could help decision-makers during volcano eruption crisis.

Acknowledgments A.C. was supported by a CONICYT postgraduate scholarship. This work has been partially funded through FONDECYT project 1040515 (PI: Andres Rivera, co-I Jorge Clavero). We thank Gabriela Anabalon who prepared some of the figures. We thank the help of Steve Schilling and Christian Huggel for kindly providing the codes LAHARZ and MSF and answering our questions. This paper has improved from critical and constructive reviews done by two anonymous reviewers.

References

Brock B, Rivera A, Casassa G, Bown F, Acuña C (2007) The surface energy balance of an active ice-covered volcano: Volcán Villarrica, southern Chile. Ann Glaciol 45:104–114

Castruccio A, Clavero J, Rivera A (2010) Comparative study of lahars generated by the 1961 and 1971 eruptions of Calbuco and Villarrica volcanoes, Southern Andes of Chile. J Volcanol Geotherm Res 190:297–311

Clavero J, Moreno H (2004) Evolution of Villarrica Volcano. In: Lara L, Clavero J (eds) Villarrica Volcano (39.5°S) Southern Andes, Chile. Servic Nac Geol Miner Bol 61:17–27

Clavero J, Godoy E, Arancibia G, Rojas C (2008) Moreno H (2008) Multiple Holocene sector collapses at Calbuco volcano, Southern Andes. IAVCEI General Assembly, Reykjavik, pp 17–22

Felpeto A, Marti J, Ortiz R (2007) Automatic GIS-based system for volcanic hazard assessment. J Volcanol Geotherm Res 166:106–116
González O (1995) Volcanes de Chile. Instituto Geográfico Militar, Santiago
Hubbard B, Sheridan M, Carrasco G, Díaz R, Rodríguez S (2007) Comparative lahar hazard mapping at volcan Citlaltepetl, Mexico using SRTM, ASTER and DTED-1 digital topographic data. J Volcanol Geotherm Res 160:99–124
Huggel C, Kääb A, Haeberli W, Krummenacher B (2003) Regional-scale GIS-models for assessment of hazards from glacier lake outbursts: evaluation and application in the Swiss Alps. Nat Hazard Earth Syst 3(6):647–662
Huggel C, Schneider D, Julio P, Delgado H, Kääb A (2007) Evaluation of ASTER and SRTM DEM data for lahar modeling: a case study on lahars from Popocatepetl volcano, Mexico. J Volcanol Geotherm Res 170(1–2):99–110
Iverson R (1997) The physics of debris flows. Rev Geophys 35(3):245–296
Iverson R, Schilling S, Vallance J (1998) Objective delineation of lahar-hazard zones downstream from volcanoes. Geol Soc Am Bull 110:972–984
Klohn E (1963) The February 1961 Eruption of Calbuco Volcano. Bull Seismol Soc Am 53(6):1435–1436
Lopez-Escobar L, Parada M, Moreno H, Frey F, Hickey-Vargas R (1992) A contribution to the petrogenesis of Osomo and Calbuco volcanoes, Southern Andes (41°00′–41°30′S): comparative study. Andean Geol 19(2):211–226
Macedonio G, Costa A, Folch A (2008) Ash fallout at Vesuvius: numerical simulations and implications for hazard assessment. J Volcanol Geotherm Res 178:366–377
Magirl CS, Griffiths PG, Webb RH (2010) Analyzing debris flows with the statistically calibrated empirical model LAHARZ in southeastern Arizona, USA. Geomorphology 119:111–124
Major J (1997) Depositional processes in large-scale debris-flow experiments. J Geol 105:345–366
Major J, Newhall C (1989) Snow and ice perturbation during historical volcanic eruptions and the formation of lahars and floods. Bull Volcanol 52:1–27
Malin M, Sheridan M (1982) Computer-assisted mapping of pyroclastic surges. Science 217:637–640
Moreno H (1993) Volcán Villarrica, Geología y evaluación del riesgo volcánico, Regiones IX y X, 39°25′S. Proyecto FONDECYT 1247 1991–1992. Santiago
Moreno H (1999) Mapa de peligros del volcán Calbuco. Región de los Lagos. Servicio Nacional de Geología y minería, Documentos de trabajo, No 12, 1 mapa escala 1:75,000. Santiago
Moreno H (2000) Mapa de peligros del volcán Villarrica, Regiones de la Araucanía y de Los Lagos. Servicio Nacional de geología y Minería, Documento de trabajo, No 17, 1 mapa escala 1:75000. Santiago
Moreno H, Clavero J (2006) Geología del área del volcán Villarrica, Regiones de la Araucanía y de los Lagos. Servicio Nacional de Geología y Minería, Carta Geológica de Chile, Serie Geología Básica, 98,1 mapa escala 1:50,000, Santiago
Moreno H, Naranjo J (2004) Calbuco volcano historic block-and-ash and pyroclastic flows: increasing threatening on surrounding communities, Southern Andes 41.5°S. IAVCEI General Assembly, Pucon, Chile, 14–19 Nov 2004
Moreno H, Naranjo J, Clavero J (2006) Generación de lahares calientes en el volcán Calbuco, Andes del Sur de Chile (41.3°S). XI Congreso Geológico Chileno, Antofagasta. Abstracts (CD)
Muñoz-Salinas E, Castillo-Rodriguez M, Manea V, Manea M, Palacios D (2009) Lahar flow simulations using LAHARZ program: application for the Popocatepetl volcano, Mexico. J Volcanol Geotherm Res 182:13–22
Naranjo J, Moreno H (2004) Laharic debris-flows from Villarrica Volcano. In: Lara L, Clavero J (eds) Villarrica Volcano (39.5°S) Southern Andes, Chile. Servic Nac Geol Miner Bol 61:28–38
Oramas Dorta D, Toyos G, Oppenheimer C, Pareschi MT, Sulpizio R, Zanchetta G (2007) Empirical modelling of the May 1998 small debris flows in Sarno (Italy) using LAHARZ. Nat Hazards 40:381–396
Patra AK, Nichita CC, Bauer AC, Pitman EB, Bursik M, Sheridan MF (2006) Parallel adaptative discontinuous Garlerkin approximation for thin layer avalanche modeling. Comput Geosci 32:912–926
Petit-Breuilh M (1999) Cronología Eruptiva Histórica de los volcanes Osorno y Calbuco, Andes del Sur (41°–41°30S). Servi Nac Geol Miner Bol 53:1–46
Pierson T, Janda R, Thouret J, Borrero C (1990) Perturbation and melting of snow and ice by the 13 November 1985 eruption of Nevado del Ruiz, Colombia, and consequent mobilization, flow and deposition of lahars. J Volcanol Geotherm Res 41:17–66
Pierson T, Major J, Amigo A, Moreno H (2013) Acute sedimentation response to rainfall following the explosive phase of the 2008–09 eruption of Chaitén Volcano. Bull Volcanol, Chile. doi:10.1007/s00445-013-0723-4

Quinteros C (1991) Estudio de los lahares del volcán Llaima-IX° Región de la Araucanía. Dissertation, Universidad de Chile

Renschler C (2005) Scales and uncertainties in volcano hazard prediction: optimizing the use of GIS land models. J Volcanol Geotherm Res 139(1–2):73–87

Rivera A, Corripio J, Brock B, Clavero J, Wendt J (2008) Monitoring ice capped active Volcán Villarrica in Southern Chile by means of terrestrial photography combined with automatic weather stations and GPS. J Glaciol 54(188):920–930

Rivera A, Zamora R, Uribe J, Wendt A, Oberreuter J, Cisternas S, Gimeno F, Clavero J (2014) Recent changes in total volume on ice on Volcan Villarrica, Southern Chile. Nat Hazards. doi:10.1007/s11069-014-1306-1

Schilling S (1998) LAHARZ: GIS programs for automated mapping of lahar-inundations hazard zones. US Geological Survey Open-File Report 98-638

Schilling S (2014) Laharz_py: GIS tools for automated mapping of lahar inundation hazard zones. US Geological Survey Open-File Report 2014-1073

Sellés D, Moreno H (2011) Geología del volcán Calbuco, Región de los Lagos. Servicio Nacional de Geología y Minería, Carta Geológica de Chile, Serie Geología Básica, 20, 1 mapa escala 1:50,000, Santiago

Stern C, Moreno H, Lopez-Escobar L, Clavero J, Lara L, Naranjo J, Parada M, Skewes M (2007) Chilean Volcanoes. In: Moreno T, Gibbons W (eds) The geology of Chile. Geological Society of London, London, pp 149–180

Stevens N, Manville V, Heron D (2002) The sensitivity of a volcanic flow model to digital elevation model accuracy: experiments with digitised map contours and interferometric SAR at Ruapehu and Taranaki volcanoes, New Zealand. J Volcanol Geotherm Res 160(1–2):99–124

Vallance J (2000) Lahars. In: Sigurdsson H (ed) Encyclopedia of volcanoes. Academic Press, San Diego, pp 601–616

Vicari A, Ciraudo A, Del Negro C, Herault A, Fortuna L (2009) Lava flow simulations using discharge rates from thermal infrared satellite imagery during the 2006 Etna eruption. Nat Hazards 50:539–550

Widiwijayanti C, Voight B, Hidayat D, Schilling SP (2009) Objective rapid delineation of areas at risk from block-and-ash pyroclastic flows and surges. Bull Volcanol 71:687–703

Worni R, Huggel C, Stoffel M, Pulgarin B (2012) Challenges of modeling current very large lahars at Nevado del Huila, Colombia. Bull Volcanol 74:309–324